*Proceedings of the 11th World Congress on Mechanical, Chemical, and Material Engineering (MCM'25)*
*Paris, France - August, 2025*
*Paper No. HTFF 256*
*DOI: 10.11159/htff25.256*

# Numerical Approach to Correct the Flow Patterns in an Electrostatic Precipitator via fitting Perfect Perforated Plate Configuration

**Masoud Darbandi[1], Armin Mohiaddini[1], Pooya Javadpoor[1], Gerry Schneider[2]**
[1]Sharif University of Technology
Sharif University of Technology, Azadi Ave, Tehran, 11365-11155, Iran
darbandi@sharif.edu, armin.mohyeddin@ae.sharif.edu, javadpoor.pooya@ae.sharif.edu
[2] University of Waterloo
University of Waterloo, 200 University Ave W, Waterloo, ON, N2L 3G1, Canada
gerrys@uwaterloo.ca

***Abstract*** **-** Electrostatic precipitators (ESPs) separate dust particles from a gas flow and play an important role in air pollution control in industries such as steel mills and coal-fired power plants. To reduce the gas flow velocity, a divergent diffuser is installed at the inlet of the electrostatic precipitator, so that the electrostatic plates have enough time to collect the dust particles. However, the diffuser often causes separation and non-uniformity of the gas flow in the inlet area, which can significantly reduce the collection efficiency in the particle collection area. Therefore, ensuring uniform gas flow distribution is essential for optimal electrostatic precipitator performance. One method of controlling the gas flow in the diffuser is to use perforated plates in the diffuser, which can prevent flow separation and create a uniform flow in the particle collection area. Several parameters affect the uniformity of the flow passing through these perforated plates, including the flow velocity, the position of the plates, and their porosity. This study investigates the effect of inlet mass flow rate, the number of perforated plates, and their placement on the flow uniformity using the computational fluid dynamics (CFD) method. The results show that these parameters significantly affect the flow uniformity, which is an indicator of system efficiency.

***Keywords*****:** Electrostatic Precipitator (ESP), Air Pollution Control, Flow Uniformity, Perforated Plates, Computational Fluid Dynamics (CFD)

## 1. Introduction

Industrial activities such as fossil fuel combustion, raw material processing, and waste incineration are the main sources of dust emissions that cause atmospheric air pollution. The dust emitted in these processes poses significant environmental and public health risks. As a result, dust emission control plays an important role in environmental and social health to reduce industrial air pollution. Electrostatic precipitators are widely used in industrial sectors due to their high efficiency in removing dust from exhaust gas streams. The performance of the electrostatic precipitator is influenced by the flow characteristics at the inlet of the particle collection zone, and the efficiency of the particulate collection increases with uniform and low-velocity inlet gas flow. To reduce the inlet flow velocity, a diverging diffuser is installed at the inlet of the electrostatic precipitator. However, adverse pressure gradients within the diffuser often cause flow separation, resulting in non-uniform velocity distribution and reduced collection performance. To address this problem, flow-regulating elements such as perforated plates are commonly used to improve flow uniformity. The effectiveness of these plates depends on various parameters, including their porosity, their position in the diffuser, and the number of plates. The study of the effect of the perforated plate parameters on flow uniformity is carried out by two methods: experimental testing of the electrostatic precipitator model and numerical simulation. Model testing to check flow uniformity provides reliable results, but can be complex and expensive, and is limited to a specific model. Numerical simulation helps to check the flow uniformity in an electrostatic precipitator and can be used to examine a variety of models, but the numerical model and numerical solver models contain simplifications that cause differences between the model testing results and the numerical simulation. For this reason, the numerical simulation results are compared with the model testing results and on-site measurements to verify their accuracy.

Electrostatic precipitators have been studied in previous research. Experiments on a Lab-scale duct and electrostatic precipitator model were conducted to investigate the effect of porosity, location, and number of perforated plates on flow uniformity. These three parameters were investigated in the experiment to determine their optimal state [1]. Numerical simulations were performed on three electrostatic precipitator models to investigate the flow distribution, and then geometric modifications were made to the models to achieve a more uniform flow distribution, which increased efficiency. The numerical results were compared with on-site measurement results, and the differences were investigated [2]. Furthermore, CFD simulations on a full-scale electrostatic precipitator were performed using simplified models to assess the flow distribution. Design modifications, including duct inserts and guide vanes, were evaluated for velocity uniformity. The simulation results were partially validated against experimental and on-site measurements [3].

## 2. Numerical Model

Figure 1 displays the 3D model of the computational domain along its side view. The computational domain consists of the inlet and outlet flow ducts, perforated plates, and particle collection zones. To reduce computational costs, the perforations in the plates and the collector plates in the particle collection zone were not explicitly modeled; instead, their effects were simulated by applying equivalent source terms. Three specific locations were selected for the perforated plates, and the number of plates at each location is indicated.

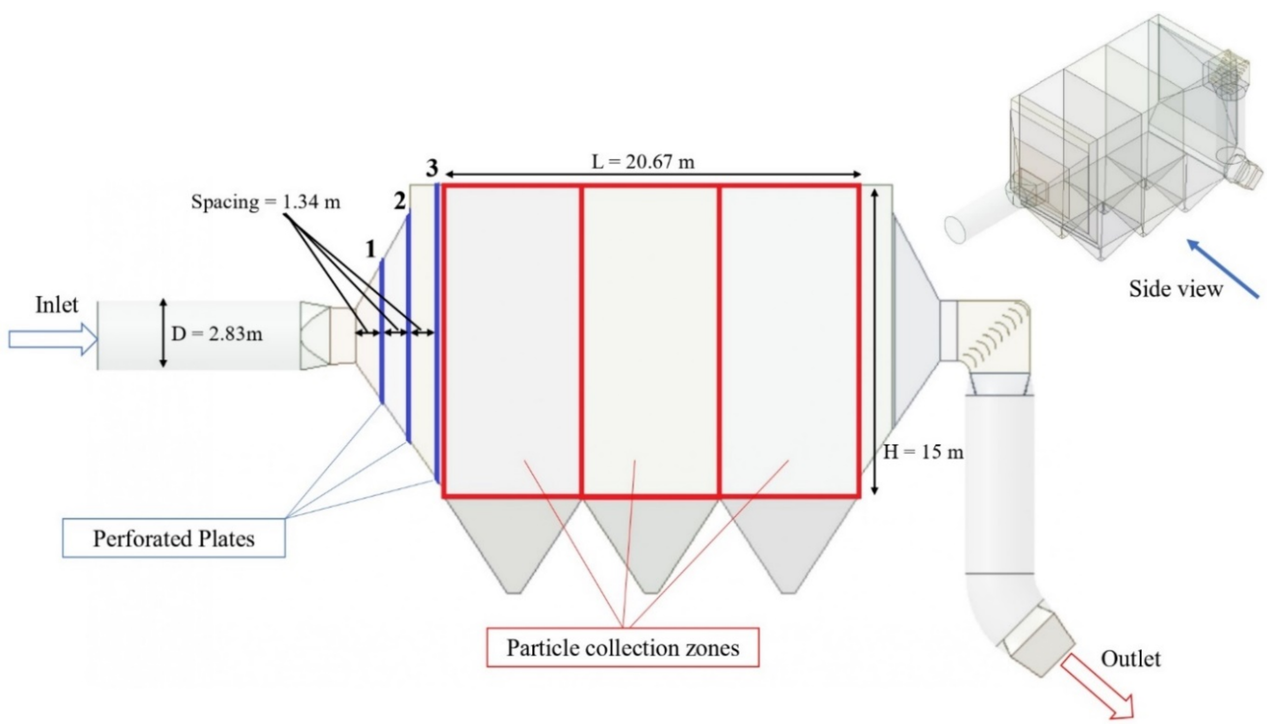


Fig. 1: Computational domain of electrostatic precipitator

### 2.1. Computational Mesh Setup

The computational domain is discretized using structured and unstructured cells. Structured elements are applied in regions where the flow behavior is important, such as near the inlet, diffuser, and collection zones, to enhance numerical simulation accuracy. Unstructured elements are applied in regions where the flow behavior has a negligible impact on results, and structured meshing is not feasible. Figure 2 shows the mesh of the computational domain, which consists of 4,009,938 cells.

To ensure the independence of the numerical solution from the computational mesh, a mesh independence study was conducted. Three cases with approximately 2,000,000, 4,000,000, and 8,000,000 cells were simulated to verify the independence of the solution from the mesh, and the total pressure drop across the electrostatic precipitator was chosen as the comparison parameter of the three cases. As shown in Table 1, the total pressure drop increased approximately 10.21% when increasing the mesh from 2,000,000 to 4,000,000 cells, but only 1.15% from 4,000,000 to 8,000,000 cells. Based on this analysis, the mesh with 4,000,000 cells was selected for the rest of simulations.

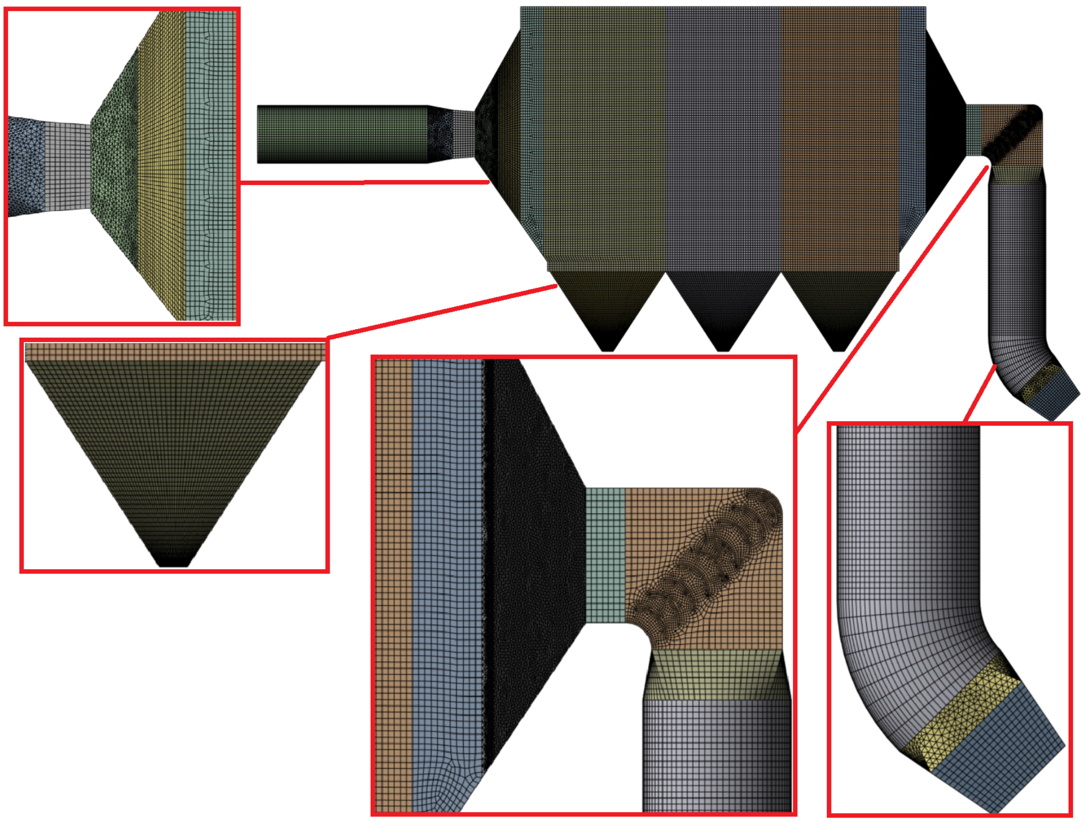

Fig. 2: Computational mesh of the electrostatic precipitator domain

Table 1: Mesh independence study showing the comparison of pressure drop at different numbers of cells.

| Approximate Number of Cells | Total pressure drop (Pa) | Relative Difference (%) |
|---|---|---|
| 2,000,000 | 140.12 | - |
| 4,000,000 | 154.46 | 10.21 |
| 8,000,000 | 156.23 | 1.15 |

## 2.2. The Governing Equations

The incompressible flow governing equations include the continuity and momentum equations as follows:

$$\frac{\partial \rho}{\partial t} + \nabla . (\rho \vec{V}) = 0 \quad (1)$$

$$\frac{\partial \vec{V}}{\partial t} + \vec{V} . \nabla \vec{V} = -\frac{\nabla P}{\partial \rho} + \nu \nabla^2 \vec{V} + \vec{g} \quad (2)$$

where $\vec{V}$ is the flow velocity vector, $\rho$ the fluid density, P the time-averaged pressure, $\nu$ the kinematic viscosity of fluid, and $\vec{g}$ the gravitational acceleration vector,. The turbulence influences are modeled using the k-epsilon realizable model, which is suitable for simulating flow separation regions and the generated vortices [5]. This model includes the displacement equation for the turbulence kinetic energy (k) and its rate of dissipation (ε). The root-mean-square (RMS) parameter is used to assess the flow uniformity as follows:

$$RMS(\%) = 100 \times \sqrt{\frac{\sum_{i=1}^{n} \left(U_i - \bar{U}\right)^2}{(n-1)\bar{U}^2}} \tag{3}$$

where n is the number of selected points of the plane, $U_i$ the local velocity of each point, and $\bar{U}$ the average velocity of the plane. This parameter is computed as the standard deviation of local velocities relative to the plane-averaged velocity. Indeed, a lower RMS value corresponds to a greater flow uniformity and enhanced flow conditioning.

### 2.3. Boundary Conditions

As shown in Figure 1, the boundary condition of the outlet is considered as a mass flow outlet to simulate the suction-driven flow downstream of the duct, and the inlet boundary condition is considered as a pressure inlet. The flow is modeled as incompressible with a constant air density of $\rho = 0.822$ kg/m$^3$. The perforated plates inside the diffuser are modeled as a pressure jump interface, with assigned pressure loss coefficients to evaluate their influence on velocity distribution. The particle collection zones are considered porous zones to investigate the pressure drop of the particle collection plates.

### 2.4. Validation

To ensure the accuracy of the pressure jump and porous zone models, the achieved numerical solutions were validated using the experimental data [4]. In the benchmark case, pressure was measured along a duct to calculate the pressure drop caused by the perforated plate placed inside the duct. A numerical simulation was performed based on the benchmark case to compare the pressure drop calculated from the numerical simulation with the experimental data. Figure 3 shows the calculated pressure drop across the perforated plate, and the maximum deviation between the numerical simulation and experimental data, which is below 10%. Several factors may result in discrepancies, e.g., the chosen numerical models. For example, the numerical model considered simplified assumptions, such as using the Reynolds-Averaged Navier-Stokes (RANS) turbulence modeling, which may not represent complex flow field behavior around the perforated plate. Additionally, the inlet boundary condition in the numerical model assumes a fully developed velocity profile, which may differ from the actual laboratory setup, where upstream piping and bends provide a non-uniform velocity profile at the inlet. Despite these factors, the error percentage of less than 10% is acceptable and confirms the accuracy of the pressure jump and porous zone models.

Based on the validation, a similar numerical approach was performed to calculate the pressure drop coefficient of the Perforated plates and the collector plates specific to this study. The pressure loss coefficients were derived numerically and used to define boundary conditions within the electrostatic precipitator domain using pressure jump and porous zone models.

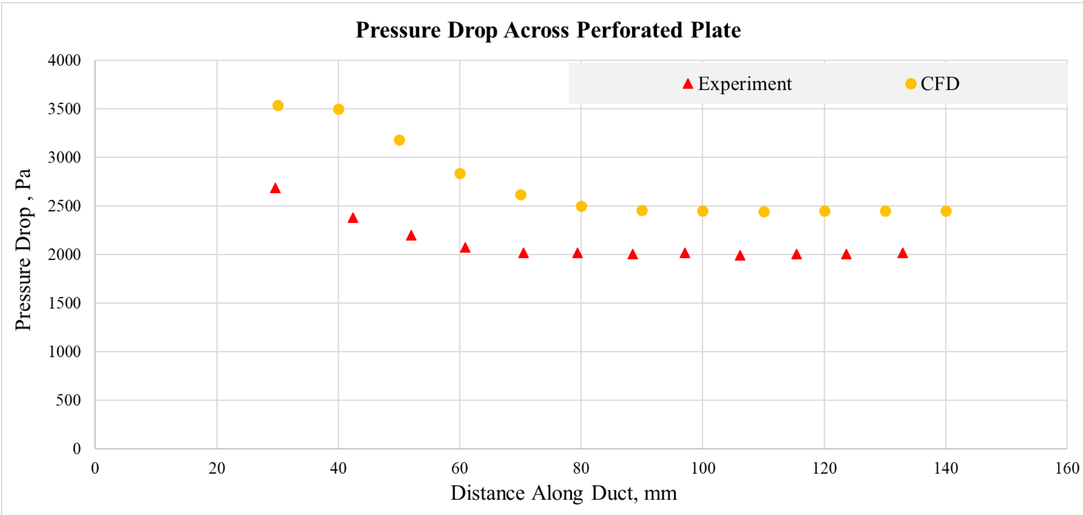

Fig. 3: The CFD validation of the pressure drop along the duct length with a perforated plate

### 2.5. Solver Settings

To ensure the credibility of the achieved numerical solutions, the computations were performed using a collocated, cell-centered FV approach and the governing equations were solved in a fully-coupled manner. The pressure interpolation was chosen the second-order and the second-order discrete schemes were used for both the convection and viscous terms in the governing equations. As the turbulence modelling part, the transport equations for the turbulence kinetic energy (k) and the turbulence dissipation rate (ε) were discretized using the first-order scheme.

## 3. The Results and Discussion

To investigate the effect of the perforated plate configurations and mass flow rate on flow uniformity and system performance, two sets of computational simulations were conducted. The impact of perforated plate configurations was assessed by simulating five cases with different numbers and locations of plates at a constant mass flow rate of 114 kg/s. Details of the plate arrangements are provided in Table 2, with plates labeled in Figure 1. The perforated plate simulation case that indicates the best flow uniformity, as quantified by RMS, was selected for the mass flow rate simulations. The effect of mass flow rate was evaluated by simulating the model at five flow rates: 75, 90, 106, 114, and 127 kg/s.

Table 2: Different case studies for five perforated plate configurations

| Case of Simulation | Perforated plate 1 | Perforated plate 2 | Perforated plate 3 |
|---|---|---|---|
| Case 1 | × | × | × |
| Case 2 | × | × | ✓ |
| Case 3 | ✓ | × | × |
| Case 4 | ✓ | × | ✓ |
| Case 5 | ✓ | ✓ | ✓ |

### 3.1. Effect of Perforated Plates Configurations on Flow Uniformity

Figure 4 shows the velocity contours at a cross-section downstream of the perforated plates, at the inlet to the particle collection zone, for the simulated cases. Case 1, without perforated plates, exhibits the most uneven flow, while adding perforated plates enhances flow uniformity, with Case 5, a full complement of plates, presenting the most uniform velocity distribution.

Table 3 quantifies this uniformity for Cases 1 to 5 using the RMS parameter. The decreasing trend of RMS shows that increasing the number of plates and optimizing their location enhances flow uniformity at the collection zone inlet and reduces vortices caused by flow separation downstream of the diffuser. These improvements cause higher system performance and increase particle collection efficiency.

Table 3: RMS for different perforated plate configurations

| Case of Simulation | Case 1 | Case 2 | Case 3 | Case 4 | Case 5 |
|---|---|---|---|---|---|
| RMS, % | 294.6 | 206.8 | 150.8 | 108.2 | 71.3 |

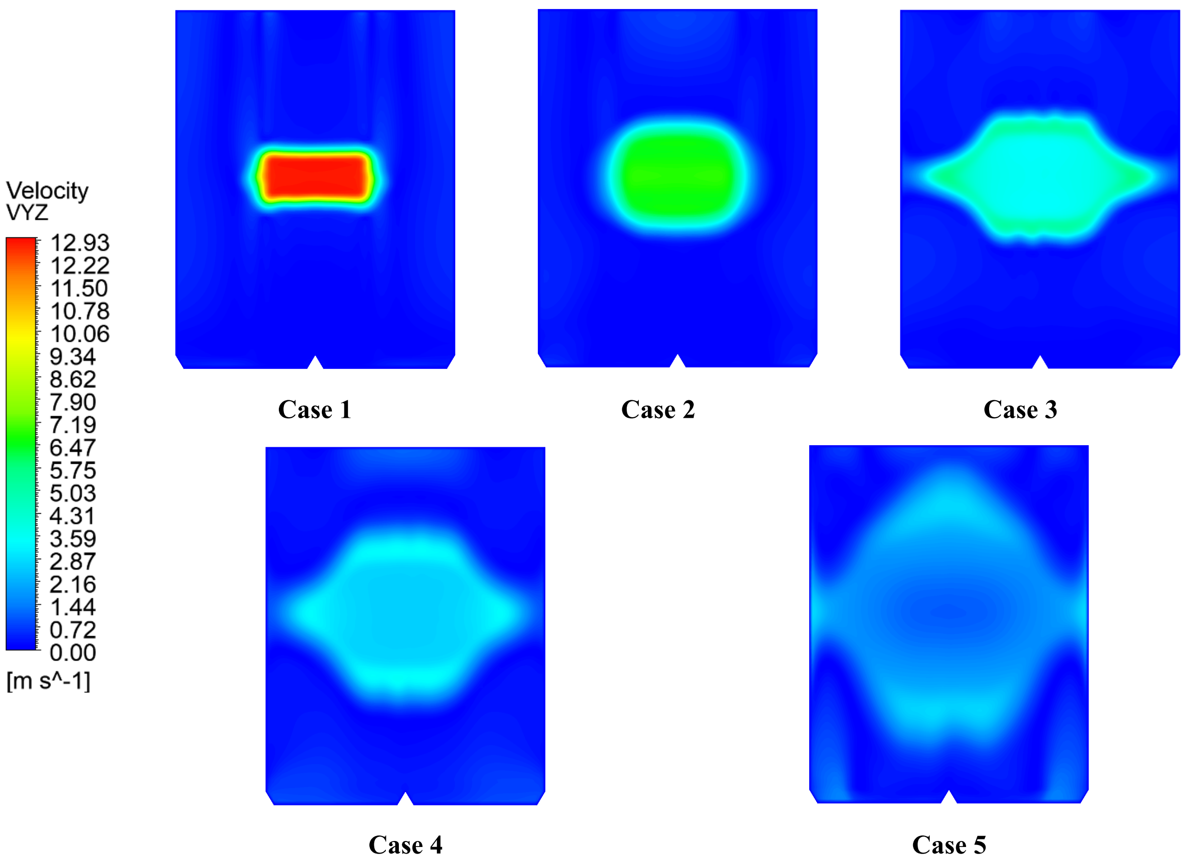


Fig. 4: Comparison of velocity contours at the collection zone inlet for five perforated plate configurations

### 3.2. Effect of Mass Flow Rate on Flow Uniformity

Case 5, with three perforated plates, was selected for the mass flow rate simulations due to its optimal flow uniformity. Figure 5 demonstrates that increasing the flow rate through the Perforated plates enhances flow distribution uniformity, as evaluated using RMS. Since the pressure drop scales with the square of the flow velocity, higher flow rates result in increased pressure drop across the perforated plates. Also, increasing the flow rate reduces particle residence time in the collection zone, which negatively affects the particle collection efficiency. Thus, the optimal operating condition for an electrostatic precipitator depends on a trade-off between flow distribution uniformity, pressure drop, and particle residence time. This trend is further illustrated in Figure 6, which shows the velocity contours at the mid-plane of the electrostatic precipitator. As the mass flow rate increases, the flow becomes more laterally distributed across the channel width, indicating a more uniform flow pattern.

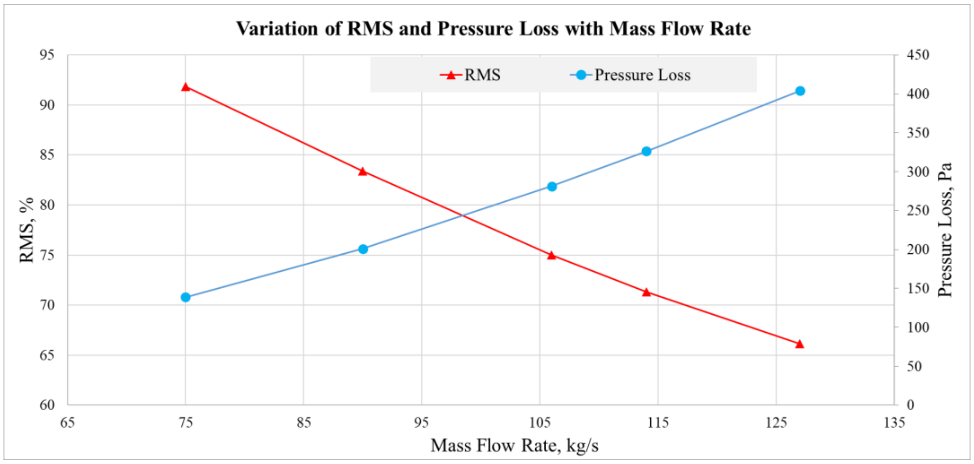

Fig. 5: Variation of RMS and pressure loss with mass flow rate

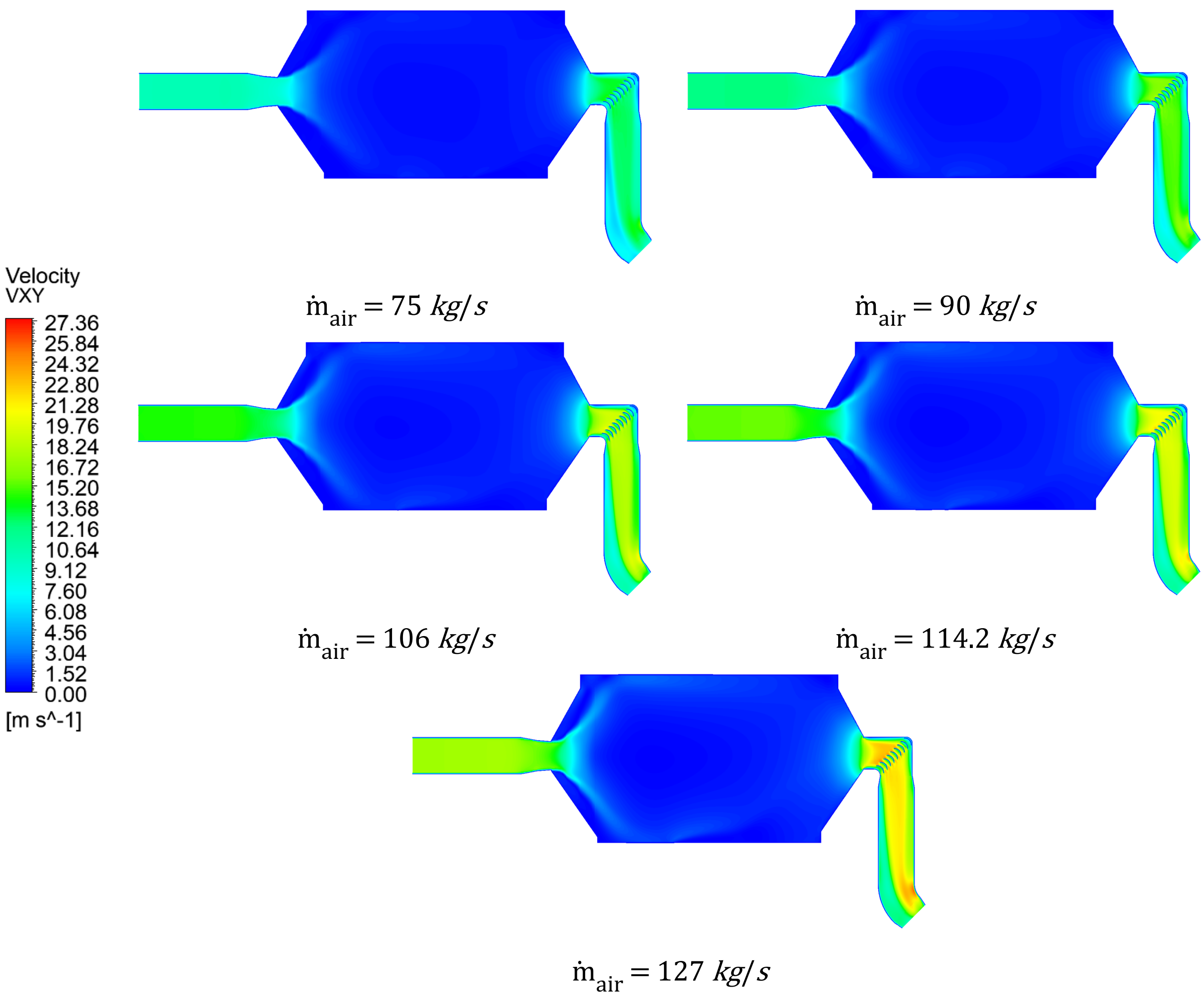

Fig. 6: Velocity contours at the mid-plane of the electrostatic precipitator for various mass flow rates

## 4. Conclusion

This study investigated the effect of the perforated plate number, placement, and the inlet mass flow rate on the flow uniformity at the particle collection zone inlet of an electrostatic precipitator. To reduce computational costs, pressure drop models were employed to simulate the effects of perforations in the plates and collector plates, with numerical results validated against experimental data, achieving an error below 10%.

- An examination of the results of five perforated plate configurations demonstrated that adding plates and optimizing their placement significantly reduces the RMS value and consequently enhances the system performance.
- In this particular electrostatic precipitator, among the five configurations studied, the use of three perforated plates with equal spacing at the electrostatic precipitator inlet yielded the best performance in flow uniformity.
- Numerical simulation results indicated that increasing the flow rate through the perforated plates enhances flow uniformity.
- As the flow rate through the perforated plates increases, the pressure drop also rises, which must be considered in the electrostatic precipitator design and selection of the optimal flow rate.

This research demonstrates that the optimal design of perforated plates plays a critical role in enhancing the performance of electrostatic precipitators. The results of this study facilitate the design of air pollution control systems in various industries.

## References


[1] D.-U. Kim, J.-T. Kim, S. H. Jeong, and S.-S. Lee, “Structure and arrangement of perforated plates for uniform flow distribution in an electrostatic precipitator,” Journal of the Air & Waste Management Association, vol. 71, no. 3, pp. 328–338, 2020.

[2] Dang Xiaoqing, Hu Hongsheng, M. Guangda, and Y. Dongjie, “Study and Application of Numerical Calculation Method for Gas Flow Distribution of Large Scale Electrostatic Precipitator,” Springer eBooks, pp. 164–168, 2009.

[3] R. Matas, M. Novák, and Jindřich Kňourek, “Numerical Simulations of Flow in Electrostatic Precipitators,” MATEC Web of Conferences, vol. 328, pp. 02021–02021, Jan. 2020.

[4] J. A. Barros Filho, M. A. Navarro, F. A. P. Magalhaesand A. A. C. dos . Santos, “Pressure drop of flow through perforated plate”. p. [7 p.], 2007.

[5] S. J. Kabadi and M. D. Hambarde, “Flow optimization of electrostatic precipitator using non-uniform porosity distribution screen,” Int. J. Curr. Eng. Technol., vol. 6, Special Issue 5, pp. 68–74, 2016.